Biomaterials 35 (2014) 7355–7362

Contents lists available at ScienceDirect

Biomaterials

journal homepage: www.elsevier.com/locate/biomaterials

An engineered 3D human airway mucosa model based on an SIS scaffold

Maria Steinke [a, b, *], Roy Gross [c], Heike Walles [a, b], Rainer Gangnus [d], Karin Schütze [d], Thorsten Walles [e]

[a] Fraunhofer Project Group Regenerative Technologies in Oncology, Röntgenring 11, 97070 Würzburg, Germany
[b] University Hospital Würzburg, Tissue Engineering and Regenerative Medicine, Röntgenring 11, 97070 Würzburg, Germany
[c] University of Würzburg, Department of Microbiology, Am Hubland, 97074 Würzburg, Germany
[d] CellTool GmbH, Am Neuland 1, 82357 Bernried, Germany
[e] University Hospital Würzburg, Department of Cardiothoracic Surgery, Oberdürrbacher Str. 6, 97080 Würzburg, Germany

ARTICLE INFO

Article history:
Received 17 March 2014
Accepted 8 May 2014
Available online 7 June 2014

Keywords:
Airway epithelium
SIS
Immunohistochemistry
TEM
Raman micro spectroscopy

ABSTRACT

To investigate interrelations of human obligate airway pathogens, such as *Bordetella pertussis*, and their hosts test systems with high in vitro/in vivo correlation are of urgent need. Using a tissue engineering approach, we generated a 3D test system of the airway mucosa with human tracheobronchial epithelial cells (hTEC) and fibroblasts seeded on a clinically implemented biological scaffold. To investigate if hTEC display tumour-specific characteristics we analysed Raman spectra of hTEC and the adenocarcinoma cell line Calu-3. To establish optimal conditions for infection studies, we treated human native airway mucosa segments with *B. pertussis*. Samples were processed for morphologic analysis. Whereas our test system consisting of differentiated epithelial cells and migrating fibroblasts shows high in vitro/in vivo correlation, hTEC seeded on the scaffold as monocultures did not resemble the in vivo situation. Differences in Raman spectra of hTEC and Calu-3 were identified in distinct wave number ranges between 720 and 1662 cm^{-1} indicating that hTEC do not display tumour-specific characteristics. Infection of native tissue with *B. pertussis* led to cytoplasmic vacuoles, damaged mitochondria and destroyed epithelial cells. Our test system is suitable for infection studies with human obligate airway pathogens by mimicking the physiological microenvironment of the human airway mucosa.

1. Introduction

Humans are the only natural hosts of *Bordetella pertussis*. These bacteria attack the airway mucosa, which leads to a severe whooping cough infection. Pertussis still is among the major health problems of the developing world. In industrial countries whooping cough is resurgent despite broad vaccination coverage [1], probably due to waning immunity and vaccine-driven evolution. To elucidate pertussis virulence mechanisms and to develop vaccines, studies with small and larger animals have been performed. The elaborated results, however, can be transferred only partially to humans [2]. Thus, to understand the complex interactions of human obligate *B. pertussis* and its host a species-specific test system for the normal airway mucosa is required. Such a test system should be well-differentiated consisting of the major airway epithelial cell types, namely basal, goblet and ciliated cells [3]. To investigate transport of bacterial toxins or other substances from the epithelial surface to the adjacent connective tissue it should display barrier properties such as tight junctions and a basement membrane. Basement membrane formation depends on different components secreted by epithelial cells and fibroblasts located in the adjacent connective tissue of the airway mucosa [4]. This is why fibroblasts should also be integrated in a test system for the normal airway mucosa.

Most airway tissue models only mimic the epithelial layer [5–8], whereas only few groups presented coculture test systems including fibroblasts seeded on synthetic membranes or collagen gels [9,10]. Our group generated a biological vascularised scaffold (BioVaSc), which was successfully implanted in human recipients

* Corresponding author. Fraunhofer Project Group Regenerative Technologies in Oncology, Röntgenring 11, 97070 Würzburg, Germany. Tel.: +49 931 31 80720; fax: +49 931 31 81068.
E-mail address: maria.steinke@igb.fraunhofer.de (M. Steinke).

http://dx.doi.org/10.1016/j.biomaterials.2014.05.031
0142-9612/

for tracheobronchial reconstruction [11–13]. Thus, this scaffold seems to provide an ideal basis and would be an approach to generate a test system for the airway mucosa.

Human airway tissue biopsies for tissue-engineered constructs may be taken during airway surgery in a macroscopically tumour-free area. To rule out tumour-specific cell de-differentiation in tissue biopsies, histological or molecular genetic analyses are performed. These processes imply tissue fixation, labelling and destruction, which make them unusable for further cell culture experiments. Based on inelastic scattering of photons at molecules, "biological fingerprints" of living cells can be analysed using Raman micro spectroscopy (Raman-MS). A strong advantage of Raman-MS resides in its non-invasive operation which keeps the samples intact and allows downstream applications. To investigate if primary human tracheobronchial epithelial cells (hTEC) used for test system generation display tumour-specific characteristics, we collected Raman spectra of hTEC and the human airway epithelium adenocarcinoma cell line Calu-3 for comparative analysis.

Our aim was to generate a 3D tissue model for the normal human airway mucosa with high in vitro/in vivo correlation consisting of the respiratory epithelium, a basement membrane and connective tissue with fibroblasts, which is suitable for infection studies with *B. pertussis* and other human obligate airway pathogens.

2. Material and methods

2.1. Donor patients

Bronchial segments for hTEC isolation were obtained from three patients undergoing elective pulmonary resection at the University Hospital Würzburg. Human primary fibroblasts were isolated from a skin biopsy. Informed consent was obtained beforehand and the study was approved by the institutional ethics committee on human research of the Julius-Maximilians-University Würzburg (vote 182/10).

2.2. Animals

For collagen scaffold generation based on the BioVaSc, which is covered by patents (Biological Vascularised Scaffold; EP1500697, DE 103 33 863), porcine jejunal segments were explanted from three 6-weeks-old domestic pigs after a standard protocol [14,15]. For test system generation, 1.5 cm^2 BioVaSc segments consisting only of small intestine submucosa without mucosa (SIS^-) were used. All animals received human care in compliance with the Guide for Care and use of Laboratory Animals published by the National Institutes of Health (NIH publication No. 85-23, revised 1996) after approval from our institutional animal protection board.

2.3. Bacteria

B. pertussis strain Tohama I [16] was grown at 37°C on Bordet-Gengou (BG) agar plates supplemented with 15% sheep blood [17] or in Stainer-Scholte (SS) liquid medium [18] as described previously [19].

2.4. Cells

All cells were cultivated under standard conditions (37°C, 5% CO_2) and cell culture media were renewed three times per week. The human airway epithelial cell line Calu-3 (ATCC HTB55, Manassas, USA) obtained from the metastatic site of lung adenocarcinoma tissue was cultivated according to the provider's instructions. To isolate hTEC from human tracheobronchial biopsies, the airway mucosa was removed mechanically, placed into plastic cell culture dishes and covered with Airway Epithelial Cell Growth Medium (AECG, catalogue #2030701, Provitro, Berlin, Germany). After 8–12 days sufficient hTEC were grown out of the tissue pieces to collect Raman spectra and to generate the test systems. Human dermal fibroblasts were cultivated in DMEM supplemented with 10% FCS.

2.5. 3D test system generation

To generate a 3D test system for the human airway mucosa, SIS^- segments were fixed between two metal cylinders. For coculture models, the scaffold was seeded with fibroblasts (100,000 cells/cm^2) from the apical side and cultivated under submerged conditions. The next day, hTEC were added (400,000 cells/cm^2) from the apical side and the whole construct was cultivated under airlift conditions for 3 weeks. Here, a cell culture medium mixture made of 50% AECG and 50% fibroblast culture medium was used. To generate monoculture 3D test systems only with hTEC, all fibroblast-associated steps described above were omitted. Generation of test systems was done in three independent experiments.

2.6. Infection studies with B. pertussis

Small segments of human native airway mucosa were placed in cell culture dishes as described for hTEC isolation and covered with a solution containing 5×10^8 *B. pertussis* in AECG. Then, the cell culture dishes were centrifuged for 3 min with 600 *g* at room temperature to accelerate bacterial adherence, followed by incubation at 37° for 6 h. Non-infected airway mucosa segments covered with AECG were treated equally and served as controls.

2.7. Histology and immunohistochemistry

For histological and immunohistochemical analysis 3D test systems were immersion-fixed in 4% formalin, embedded in paraffin and sectioned at 3 μm thickness. Then, samples were deparaffinised in xylene and rehydrated in a graded series of ethanol. According to standard protocols haematoxylin & eosin staining for general morphological assessment and Alcian blue staining to detect mucus were performed. For immunohistochemical staining antigen retrieval was performed in a steamer at pH 6 to detect Vimentin and at pH 9 to detect Cytokeratin 5 (CK5) and Cytokeratin 18 (CK18). Endogenous peroxidases were inactivated using 3% H_2O_2. Samples were incubated for 1 h at room temperature with one of the following primary antibodies diluted in antibody incubation buffer (catalogue #ALI20R500, DCS Innovative Diagnostik-Systeme, Hamburg, Germany): monoclonal mouse Anti-Human-CK 5/6 (1:200, catalogue #M7237, Dako Cytomation, Hamburg, Germany), monoclonal mouse Anti-Human-CK 18 (1:100, catalogue #M7010, Dako Cytomation), monoclonal mouse Anti-Human-Vimentin (1:1000, catalogue #ab8069, Abcam, Cambridge, UK). Excess primary antibodies were removed by washing. Detection of bound primary antibodies and chromogenic visualisation with 3′3′-Diamonobenzidine were carried out using DCS Super Vision 2 HRP-Polymer-Kit (catalogue #PD000KIT, DCS Innovative Diagnostik-Systeme) according to manufacturer's instructions. Sections were counterstained with Maier's haematoxylin and blued in tap water. Samples were dehydrated in ethanol, cleared in xylene and coverslipped. To control specificity of primary antibodies negative controls (omission of primary antibodies) were performed for each experiment. Stained tissue samples were evaluated with an Axio Lab.A1 (Zeiss, Jena, Germany) and photographs were taken using the BZ-9000 BIOREVO System (Keyence, Neu-Isenburg, Germany).

2.8. Transmission electron microscopy

For ultrastructural analysis of 3D test systems and native human airway mucosa segments after infection with *B. pertussis*, samples were immersion-fixed in 1% formalin and 4.5% glutaraldehyde. After extensive washing samples were incubated in 2% osmium tetroxide, dehydrated in ethanol and embedded in Epon resin. Ultrathin sections (74 nm), were cut, placed onto grids, contrasted with uranyl acetate and lead citrate [20] and examined with a transmission electron microscope (LEO AB 912, Zeiss). All pictures were assembled and adjusted for brightness and contrast in Adobe Photoshop CS.

2.9. Raman micro spectroscopy of living airway epithelial cells

Calu-3 and hTEC, which were used for test system generation, were seeded on cell culture dishes with glass bottom. Cell culture medium was replaced every second day. At approximately 70% confluence cell culture medium was replaced by fresh AECG immediately before Raman measuring to exclude the impact of cell culture medium-related Raman spectra. To collect Raman spectra we used the BioRam system (CellTool GmbH, Bernried, Germany) with a non-destructive 785 nm diode laser. This system combines Raman spectrometry with digital microscopy and was calibrated using standard silicon samples. All molecules within the laser focus contribute to a sum spectrum resulting in a unique fingerprint. To obtain a reliable data set, for each cell type 100 cells were selected under bright-field illumination and pinpointed for automatic spectra retrieval. Raman spectra were taken from the cytoplasm using accumulated scans of 4×10 s and an excitation power of 80 mW.

2.10. Raman data pre-treatment and multivariate data analysis

Data were processed applying customised software (CellTool). First, spectra were cropped to the wave number region between 400 and 1700 cm^{-1} representing a range with high amount of biological information [21] and baseline correction with asymmetric least squares smoothing was applied [22]. Further data pre-treatment with a median filter for noise reduction, unit vector normalisation and subsequent multivariate data analysis were done with the statistical software The Unscrambler X 10.3 (Camo Software, Oslo, Norway). We performed Principle Component Analysis (PCA) using the NIPALS algorithm and cross validation, which is a common procedure for spectral data analysis. In 200 samples, three outliers were identified and removed.

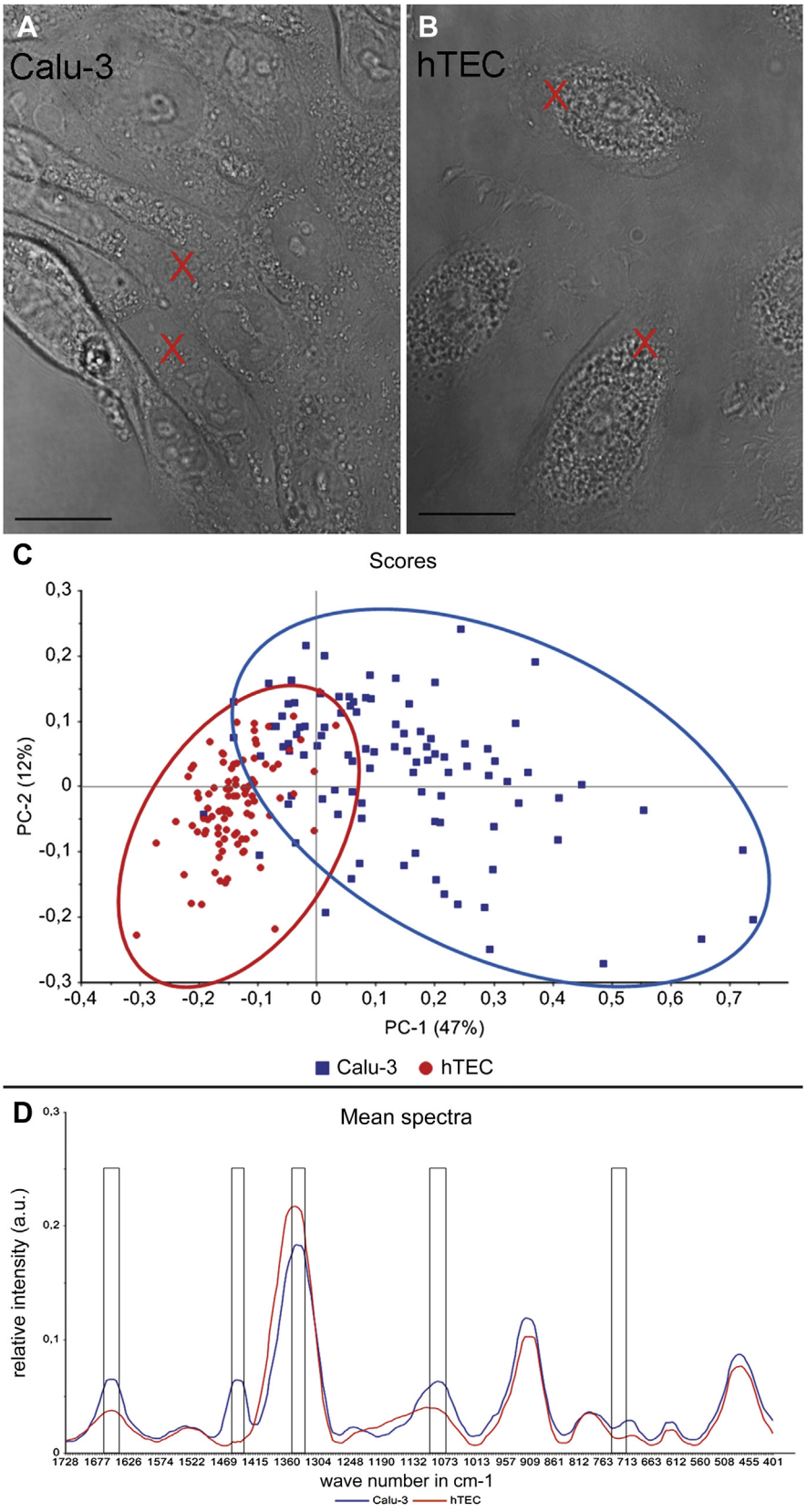

Fig. 1. Light micrographs of Calu-3 (A) and hTEC (B) at the Raman micro spectroscope. Red crosses exemplarily show measuring positions in the cytoplasm; scale bars: 20 μm. The scores plot (C) shows cell type-specific data separation on PC1. (D) illustrates mean spectra of hTEC (red) and Calu-3 datasets (blue). Framed areas indicate wave number ranges, which are relevant for data separation.

3. Results

3.1. Raman-MS of Calu-3 and hTEC

We collected Raman spectra in the cytoplasm of the human airway adenocarcinoma cell line Calu-3 and isolated hTEC (Fig. 1A,B). The scores plot resulting after PCA shows two cell type-specific clusters, which can be separated on PC1 (47%) with relatively broad spreading of Calu-3 data points and a small overlapping of both clusters (Fig. 1C). Mean spectra plots (Fig. 1D) were generated to compare spectra of both cell types to each other. To check if a certain wave number area was relevant for cell type-specific data separation we re-analysed the PCA on this dataset. If the scores plot showed the same or even a better split including a percentage value on PC1 bigger than 47%, this wave number area would be of high relevance. Therefore, one can clearly identify the wave numbers showing the relevant differences of the datasets. Relevant intensities with PC1 values bigger than 93% were detected at 720–725, 1073–1087, 1334–1351, 1445–1450 and 1646–1662 cm^{-1} (Fig. 2). Intensities were greater for Calu-3 at 720–725, 1073–1087, 1445–1450 and 1646–1662 cm^{-1} and greater for hTEC at 1334–1351 cm^{-1} as illustrated in the mean spectra plot (Fig. 1D).

3.2. Light microscopic and ultrastructural characterisation of the 3D test system

As only hTEC were seeded on the SIS^{-} (monoculture), the cells remained on the scaffold's surface and were distributed in a non-polarised and diffuse pattern (Fig. 3A) without mucus production (Fig. 3B). A certain amount of hTEC was CK 5- (Fig. 4A) or CK 18-positive (Fig. 4B), however, the spatial arrangement did not resemble the in vivo situation, at all (compare with online Supplementary Fig. 1). In coculture samples with hTEC and

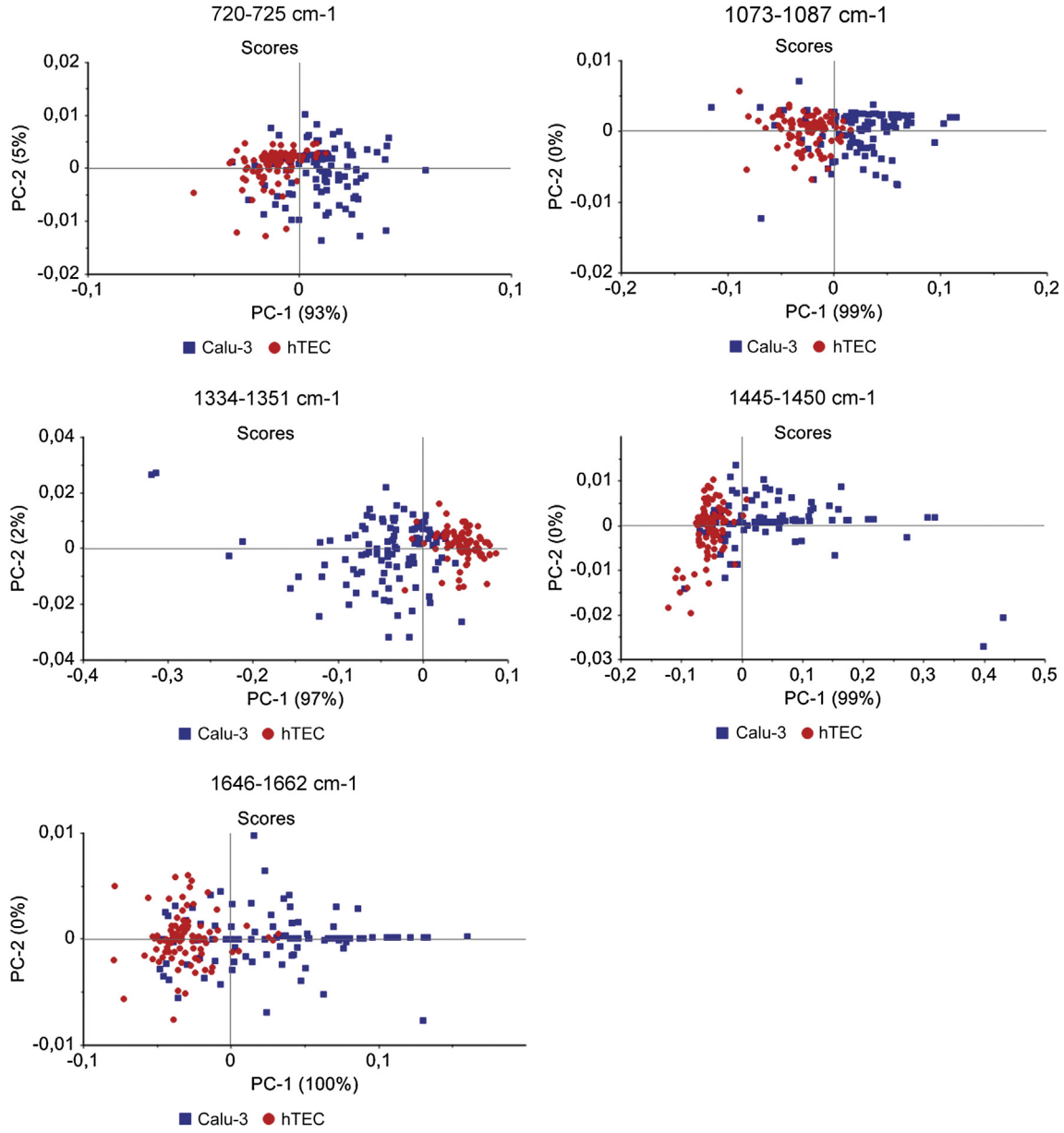

Fig. 2. PCA re-analysis showing scores plots of wave number areas relevant for cell type-specific data separation with PC1 values bigger than 93%.

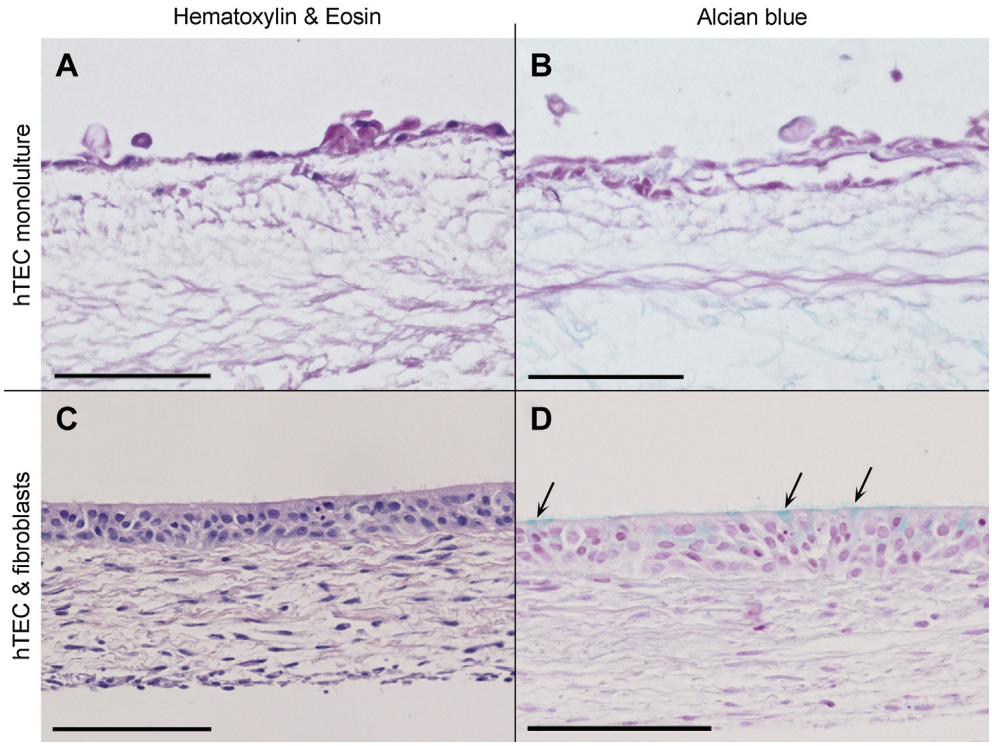

Fig. 3. Light micrographs of hTEC in mono- (A, B) and coculture with fibroblasts (C, D). Haematoxylin & eosin staining (A, C) shows general morphology and Alcian blue staining (B, D) indicates mucus production (arrows). Scale bars: 100 μm.

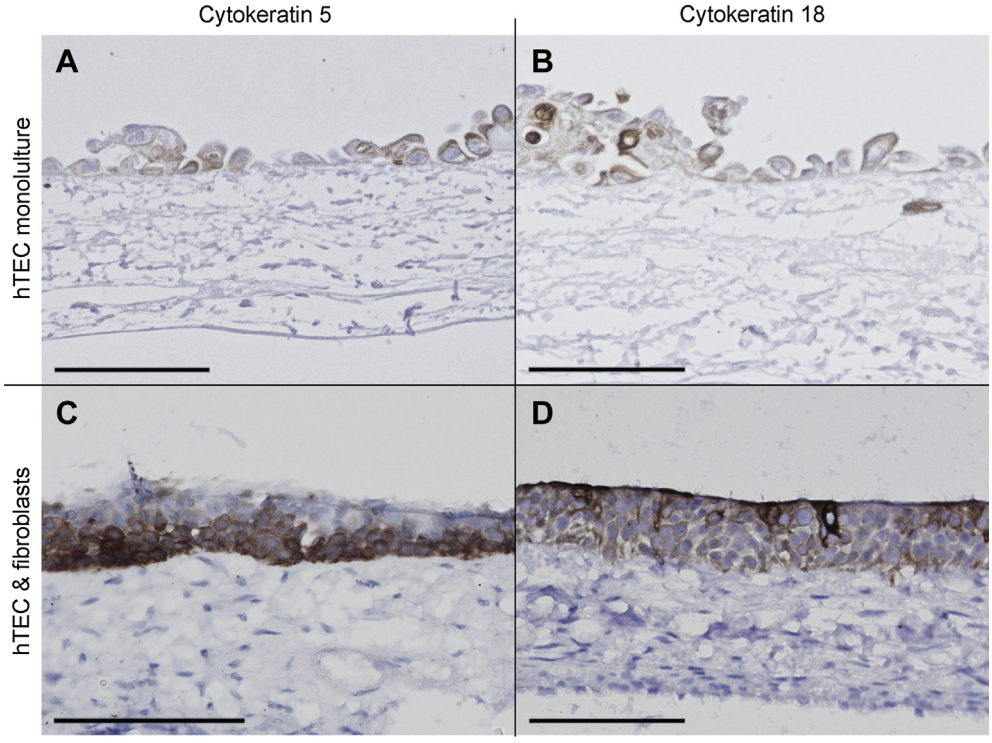

Fig. 4. Light micrographs of hTEC in mono- (A, B) and coculture with fibroblasts (C, D). Cytokeratin 5 and 18 immunoreactivity shows undifferentiated (A, C) and differentiated epithelial cells (B, D), respectively. Scale bars: 100 μm.

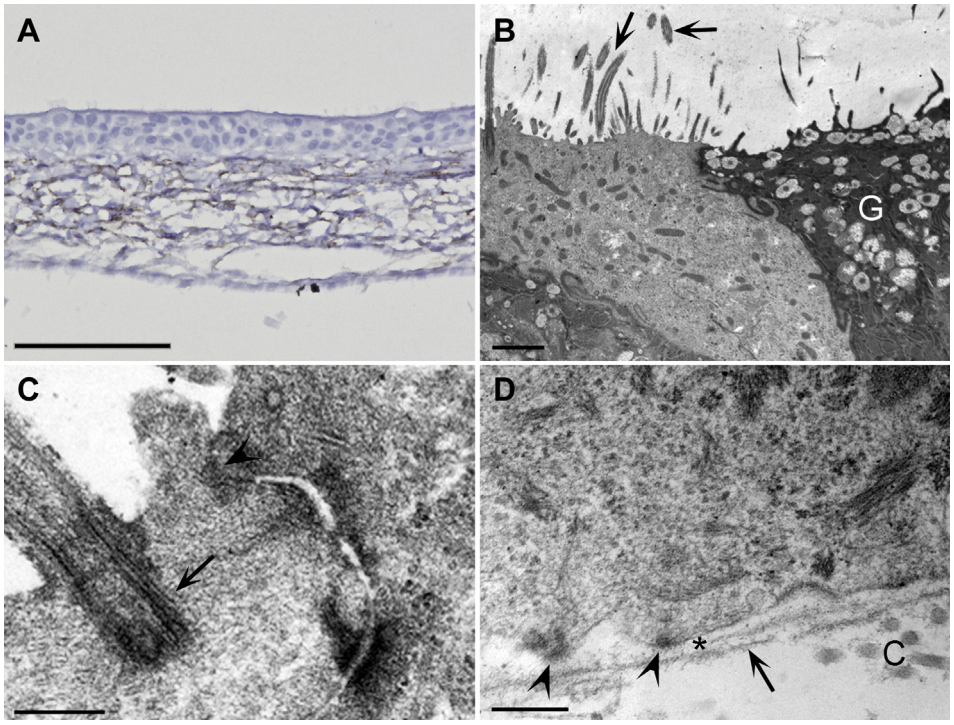

Fig. 5. Light micrograph (A) and ultrastructural analysis (B–D) of hTEC in coculture with fibroblasts. Vimentin-positive cells indicate fibroblasts (A). On the epithelial surface kinocilia (arrows in B and C) and tight junctions (arrowhead in C) were verified. Arrow in (D) points to the *lamina densa*, arrowheads to hemidesmosomes and asterisk indicates *lamina lucida*. C: collagen, G: goblet cell; scale bars: (A) 100 μm, (B) 1500 nm, (C, D) 250 nm.

fibroblasts, hTEC morphology completely differed from that observed in corresponding monocultures. HTEC formed a polarised epithelial layer (Fig. 3C) and mucus production was observed (arrows in Fig. 3D). Moreover, we documented CK 5- (Fig. 4C), and CK 18-positive cells (Fig. 4D), which were predominantly located on the basolateral and apical compartment of the epithelial layer, respectively. Using vimentin immunohistochemistry cells with mesenchymal character, such as fibroblasts, are stained. We

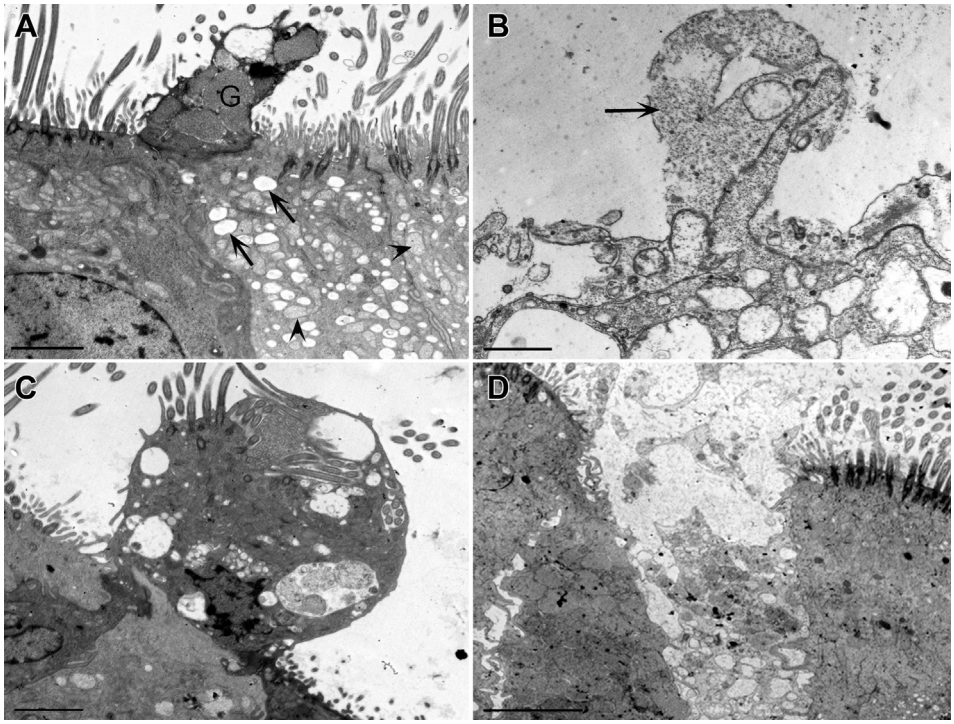

Fig. 6. Ultrastructural analysis of human airway mucosa after infection with *Bordetella pertussis*. Arrows in (A) indicate cytoplasmic vacuoles, arrowheads point to damaged mitochondria; arrow in (B) shows cytoplasmic blebbing. G: goblet cell. Scale bars: (A, C) 2000 nm, (B, D) 1000 nm.

observed that exclusively vimentin-positive cells have migrated into the scaffold (Fig. 5A). No vimentin-positive cells were seen in the epithelial region of the test system, which resembles the in vivo situation (compare with online Supplementary Fig. 1b).

On a light microscopic level, we observed fine structures on the epithelial surface, which we verified as kinocilia in TEM analysis due to the typical arrangement of microtubules (arrows in Fig. 5B) and basal bodies (arrow in Fig. 5C). Moreover, goblet cells (Fig. 5B) and tight junctions (arrowhead in Fig. 5C) were verified. At the basal compartment of the epithelium we observed hemidesmosomes located on basal cells (arrowheads in Fig. 5D) anchoring via the lamina lucida (asterisk in Fig. 5D) to the lamina densa (arrow in Fig. 5D), which are important components of the basement membrane. Next to these structures, collagen fibrils of the biological scaffold were located (Fig. 5D). All ultrastructural observations closely resemble the in vivo situation (compare with online Supplementary Fig. 2). Neither in light nor in electron microscopic samples tumour-like tissue morphology was observed.

3.3. Infection of native human airway mucosa with B. pertussis

After infection with *B. pertussis*, we qualitatively analysed human bronchus segments on an ultrastructural level. In a high amount of epithelial cells, cytoplasmic vacuoles and damaged mitochondria (Fig. 6A) were seen. We frequently observed cytoplasmic blebbing (Fig. 6B), extruded goblet and epithelial cells (Fig. 6A and C, respectively) and completely destroyed epithelial cells (Fig. 6D). Any of the morphological changes after infection with *B. pertussis* described here were observed in control samples.

4. Discussion

We generated a 3D test system for the normal human airway mucosa with high in vitro/in vivo correlation. The test system consists of a well-differentiated airway epithelium including basal cells, mucus-producing goblet cells and ciliated cells, which are important prerequisites for mucociliary clearance. Especially for infection studies with *B. pertussis* the presence of kinocilia is essential since these bacteria specifically adhere to ciliated epithelial cells [2]. The epithelium of our test system is equipped with tight junctions and is anchored via hemidesmosomes found on basal cells to a basement membrane adjacent to the SIS^{-}. The scaffold contains fibroblasts, which morphologically resembles the *lamina propria* of the airway mucosa in vivo. Moreover, the test system remains viable for up to three weeks, which is an important feature for long-term studies.

Comparing mono- and coculture test systems, we confirmed the extensive impact of fibroblasts on epithelial cell differentiation previously reported by others [10]. It is known that several factors secreted by fibroblasts, such as HGF, promote bronchus epithelial cell proliferation and differentiation [23,24]. Using very complex cell culture media, probably containing these essential factors in combination with airlift conditions, fibroblasts can be omitted to generate well-differentiated tissue models for the respiratory epithelium [7]. However, for further para- and transepithelial transport studies a 3D test system including the airway epithelium, a basement membrane and the adjacent connective tissue with fibroblasts with higher in vitro/in vivo correlation will be required.

To generate the test system, we used primary human dermal fibroblasts. Investigations with rat cells have shown that airway mucosa tissue model generation with dermal fibroblasts led to an epidermis-like morphology of airway epithelial cells [25]. However, our data on human cells do not confirm these observations, however, clearly show that our coculture test system closely resembles the in vivo situation. These different observations might be species-specific supporting our approach to avoid animal models to investigate human obligate pathogens.

Using human airway mucosa segments, we established optimal conditions for infection with *B. pertussis* since we could reproduce characteristic findings observed previously [26]. Cytoplasmic vacuoles and damaged mitochondria are associated with (reversible) necrotic processes; cytoplasmic blebbing indicate extensive cell damage. It is possible that the tracheal cytotoxin produced by *B. pertussis* is a cause of these effects [26]. Thus, we established a reliable basis for upcoming infection studies with *B. pertussis* on our 3D test system.

Comparing Raman spectra of living hTEC and the human airway epithelium adenocarcinoma cell line Calu-3 relevant differences were identified in distinct wave number ranges between 720 and 1662 cm^{-1}. Over the entire wave number range we observed two clusters for hTEC and Calu-3 using multivariate data analysis. The relatively broad data spreading of Calu-3 could indicate cell type inhomogeneity. The area where both clusters overlap indicates common features, which is not surprising since both cell types are human airway epithelial cells. In our PCA reanalysis, we detected relevant cell type-specific differences at 1073–1087, 1445–1450 and 1646–1662 cm^{-1}, which have previously been described as significant wave number ranges to discriminate human tumour tissue from normal airway and other tissue [21,27–30]. These Raman peaks are, for instance, assigned to collagen (1073–1087, 1445–1450, 1646–1662 cm^{-1}), lipids (1073–1087, 1445–1450, 1646–1662 cm^{-1}), proteins (1073–1087, 1445–1450, 1646–1662 cm^{-1}) and DNA/RNA components (1073–1087, 1646–1662 cm^{-1}) [21]. We detected further differences between hTEC and Calu-3, which are, for instance, assigned to collagen, lipids, tryptophan, glucose (1334–1351 cm^{-1}) and DNA/RNA components (720–725, 1334–1351 cm^{-1}), however, are not explicitly described in literature as tumour-specific differences. Since no tumour-associated Raman peaks and no tumour-like morphology was observed in subsequent histological analysis of 3D test systems we conclude that Raman-MS is a suitable method to investigate if vital hTEC are suitable for 3D test system generation or should be discarded due to tumour-specific characteristics.

In upcoming studies, we will use our test system to elucidate pertussis virulence mechanisms including para- and transepithelial transport of bacterial toxins. Here, intact barriers, such as tight junctions and basement membranes are necessary to assure high in vitro/in vivo correlation. Thus, in addition to our morphological observations documenting tight junctions and a basement membrane, further characterisation of barrier integrity of our test system will be performed by appropriate measurements such as the transepithelial resistance.

5. Conclusions

The usage of SIS^{-} segments obtained from the BioVaSc represents a strategy to generate 3D airway test systems. Since the scaffold was successfully implanted during tracheobronchial reconstruction in humans, our methodical procedure for test system generation additionally seems to be a promising strategy to produce clinically applicable airway patches with autologous airway epithelial cells and fibroblasts in vitro to reconstruct complex airway defects. Non-invasive Raman analysis is a powerful tool to analyse autologous cells with respect to tumour-specific characteristics and, additionally, would be useful to investigate consequences after infection of 3D test systems with *B. pertussis*.

Acknowledgements

This work was financially supported by the DFG (WA 1649/3-1) and by the European Union's Seventh Programme for Research, Technological Development and Demonstration under grant agreement No 279288 (IDEA). We thank Matthias Schweinlin, Sebastian Kress, David Fecher and Sabine Wilhelm for BioVaSc generation, Christa Amrehn, Sabine Graiff and Susanne Bauer for excellent technical assistance, Dr. Ulrich Pschirrer for providing the foreskin biopsy and Prof. Waltraud Kessler for assistance with multivariate data analysis.

Appendix A. Supplementary data

Supplementary data related to this article can be found online at http://dx.doi.org/10.1016/j.biomaterials.2014.05.031.

References

[1] Mills KH, Ross PJ, Allen AC, Wilk MM. Do we need a new vaccine to control the re-emergence of pertussis? Trends Microbiol 2014;22:49–52.
[2] van der Ark AA, Hozbor DF, Boog CJ, Metz B, van den Dobbelsteen GP, van Els CA. Resurgence of pertussis calls for re-evaluation of pertussis animal models. Expert Rev Vaccines 2012;11:1121–37.
[3] Berube K, Prytherch Z, Job C, Hughes T. Human primary bronchial lung cell constructs: the new respiratory models. Toxicology 2010;278:311–8.
[4] Knight DA, Holgate ST. The airway epithelium: structural and functional properties in health and disease. Respirology 2003;8:432–46.
[5] Bernacki SH, Nelson AL, Abdullah L, Sheehan JK, Harris A, Davis CW, et al. Mucin gene expression during differentiation of human airway epithelia in vitro. Muc4 and muc5b are strongly induced. Am J Respir Cell Mol Biol 1999;20:595–604.
[6] de Jong PM, van Sterkenburg MA, Hesseling SC, Kempenaar JA, Mulder AA, Mommaas AM, et al. Ciliogenesis in human bronchial epithelial cells cultured at the air-liquid interface. Am J Respir Cell Mol Biol 1994;10:271–7.
[7] Prytherch Z, Job C, Marshall H, Oreffo V, Foster M, BeruBe K. Tissue-specific stem cell differentiation in an in vitro airway model. Macromol Biosci 2011;11:1467–77.
[8] Yamaya M, Finkbeiner WE, Chun SY, Widdicombe JH. Differentiated structure and function of cultures from human tracheal epithelium. Am J Physiol 1992;262:L713–24.
[9] Choe MM, Sporn PH, Swartz MA. Extracellular matrix remodeling by dynamic strain in a three-dimensional tissue-engineered human airway wall model. Am J Respir Cell Mol Biol 2006;35:306–13.
[10] Pohl C, Hermanns MI, Uboldi C, Bock M, Fuchs S, Dei-Anang J, et al. Barrier functions and paracellular integrity in human cell culture models of the proximal respiratory unit. Eur J Pharm Biopharm 2009;72:339–49.
[11] Macchiarini P, Walles T, Biancosino C, Mertsching H. First human transplantation of a bioengineered airway tissue. J Thorac Cardiovasc Surg 2004;128:638–41.
[12] Mertsching H, Walles T, Hofmann M, Schanz J, Knapp WH. Engineering of a vascularized scaffold for artificial tissue and organ generation. Biomaterials 2005;26:6610–7.
[13] Walles T, Giere B, Hofmann M, Schanz J, Hofmann F, Mertsching H, et al. Experimental generation of a tissue-engineered functional and vascularized trachea. J Thorac Cardiovasc Surg 2004;128:900–6.
[14] Linke K, Schanz J, Hansmann J, Walles T, Brunner H, Mertsching H. Engineered liver-like tissue on a capillarized matrix for applied research. Tissue Eng 2007;13:2699–707.
[15] Schanz J, Pusch J, Hansmann J, Walles H. Vascularised human tissue models: a new approach for the refinement of biomedical research. J Biotechnol 2010;148:56–63.
[16] Weiss AA, Falkow S. Genetic analysis of phase change in Bordetella pertussis. Infect Immun 1984;43:263–9.
[17] Bordet J, Gengou O. L'endotoxine coqueluche use. Ann l'Institut Pasteur (Paris) 1909;23:415–9.
[18] Stainer DW, Scholte MJ. A simple chemically defined medium for the production of phase I Bordetella pertussis. J Gen Microbiol 1970;63:211–20.
[19] Fuchs TM, Deppisch H, Scarlato V, Gross R. A new gene locus of Bordetella pertussis defines a novel family of prokaryotic transcriptional accessory proteins. J Bacteriol 1996;178:4445–52.
[20] Reynolds ES. The use of lead citrate at high pH as an electron-opaque stain in electron microscopy. J Cell Biol 1963;17:208–12.
[21] Movasaghi Z, Rehman S, Rehman IU. Raman spectroscopy of biological tissues. Appl Spectrosc Rev 2007;42:493–541.
[22] Peng J, Peng S, Jiang A, Wei J, Li C, Tan J. Asymmetric least squares for multiple spectra baseline correction. Anal Chim Acta 2010;683:63–8.
[23] Myerburg MM, Latoche JD, McKenna EE, Stabile LP, Siegfried JS, Feghali-Bostwick CA, et al. Hepatocyte growth factor and other fibroblast secretions modulate the phenotype of human bronchial epithelial cells. Am J Physiol 2007;292:L1352–60.
[24] Skibinski G, Elborn JS, Ennis M. Bronchial epithelial cell growth regulation in fibroblast cocultures: the role of hepatocyte growth factor. Am J Physiol 2007;293:L69–76.
[25] Kobayashi K, Suzuki T, Nomoto Y, Tada Y, Miyake M, Hazama A, et al. Potential of heterotopic fibroblasts as autologous transplanted cells for tracheal epithelial regeneration. Tissue Eng 2007;13:2175–84.
[26] Wilson R, Read R, Thomas M, Rutman A, Harrison K, Lund V, et al. Effects of Bordetella pertussis infection on human respiratory epithelium in vivo and in vitro. Infect Immun 1991;59:337–45.
[27] Huang Z, McWilliams A, Lui H, McLean DI, Lam S, Zeng H. Near-infrared Raman spectroscopy for optical diagnosis of lung cancer. Int J Cancer 2003;107:1047–52.
[28] Lau DP, Huang Z, Lui H, Man CS, Berean K, Morrison MD, et al. Raman spectroscopy for optical diagnosis in normal and cancerous tissue of the nasopharynx-preliminary findings. Lasers Surg Med 2003;32:210–4.
[29] Liu CH, Das BB, Sha Glassman WL, Tang GC, Yoo KM, Zhu HR, et al. Raman, fluorescence, and time-resolved light scattering as optical diagnostic techniques to separate diseased and normal biomedical media. Journal of photochemistry and photobiology B. Biology 1992;16:187–209.
[30] Mahadevan-Jansen A, Mitchell MF, Ramanujam N, Malpica A, Thomsen S, Utzinger U, et al. Near-infrared Raman spectroscopy for in vitro detection of cervical precancers. Photochem Photobiol 1998;68:123–32.